Charged residue alterations in the inner-core domain and carboxy-terminus of α-tropomyosin differentially affect mouse cardiac muscle contractility

Robert D. Gaffin[1], Carl W. Tong[1], David C. Zawieja[1], Timothy E. Hewett[2], Raisa Klevitsky[2], Jeffrey Robbins[2] and Mariappan Muthuchamy[1]

[1]*336 Reynolds Medical Building, Cardiovascular Research Institute and Department of Medical Physiology, College of Medicine, Texas A & M University System Health Science Center, College Station, TX 77843-1114, USA*
[2]*Division of Molecular Cardiovascular Biology, Cincinnati Children's Hospital, Cincinnati, OH 45229-3039, USA*

Two important charge differences between the α- and β-tropomyosin (TM) isoforms are the exchange of a serine residue in the inner-core region at position 229, and a histidine residue at the carboxy-terminal end at position 276, with glutamic acid and asparagine, respectively. We have recently shown that altering these two residues in α-TM to their β-TM counterparts in transgenic (TG) mouse hearts causes a depression in both $+d P/d t$ and $-d P/d t$ and a decrease in calcium sensitivity. In this study, we address whether independent charge changes at these two residues in α-TM modulate cardiac function differentially. To test this hypothesis we generated two TG lines: α-TMSer229Glu and α-TMHis276Asn. Molecular analyses show that 98% of native α-TM is replaced by mutated protein in α-TM229 hearts whereas α-TM276 hearts show 82% replacement with the mutated protein. Isolated working heart data show that α-TM229 TG hearts exhibit a significant decrease in both $+d P/d t$ (7%) and $-d P/d t$ (8%) compared with nontransgenics (NTGs) and time to peak pressure (TPP) is also reduced in α-TM229 hearts. α-TM276 hearts show a decrease only in $-d P/d t$ (14%) and TPP is increased. pCa^{2+}–tension relationships in skinned fibre preparations indicate decreased calcium sensitivity in α-TM229 but no change in α-TM276 preparations. Force–$[Ca^{2+}]_{IC}$ measurements from intact papillary fibres indicate that α-TM276 fibres produce more force per given $[Ca^{2+}]_{IC}$ when compared to NTG fibres, while α-TM229 fibres produce less force per given $[Ca^{2+}]_{IC}$. These data demonstrate that changing charged residues at either the inner-core domain or the carboxyl end of TM alters sarcomeric performance differently, suggesting that the function of TM is compartmentalized along its length.

(Received 24 June 2004; accepted after revision 13 October 2004; first published online 14 October 2004)
Corresponding author M. Muthuchamy: 336 Reynolds Medical Building, Cardiovascular Research Institute and Department of Medical Physiology, College of Medicine, Texas A & M University System Health Science Center, College Station, TX 77843-1114, USA. Email: marim@tamu.edu

Tropomyosin (TM) is a dimeric, coiled-coil protein involved in calcium-mediated contraction of striated muscle. In order for TM to achieve its steric and allosteric effects that either prevent or allow actomyosin crossbridge formation, TM must interact with other thin filament proteins, such as the troponin (Tn) complex and actin. These interactions are largely the result of ionic forces between oppositely charged amino acids or, as postulated to occur between TM and actin, via magnesium salt bridges between residues of the same charge (McLachlan & Stewart, 1976).

Charged residues also aid in the formation of TM's dimer complex since they occupy the e and g positions of TM's heptad repeat. These residues contain ionic and polar side chains that form salt bridges between TM's two monomers (McLachlan & Stewart, 1975). In addition, TM–actin binding via TM's 14 quasi-equivalent zones, as revealed by Fourier analysis (Stewart & McLachlan, 1975; McLachlan & Stewart, 1976; Parry, 1976), is mediated by charged amino acids. Each zone contains both negatively charged and positively charged residues clustered in regions that correspond to either the 'off' or 'on' state of crossbridge activation (McLachlan & Stewart, 1976).

We have previously shown that exchanging the β-TM protein for endogenous α-TM protein in cardiac muscle alters the sarcomeric function (Muthuchamy *et al.* 1995;

 DOI: 10.1113/jphysiol.2004.070631

Palmiter *et al.* 1996; Muthuchamy *et al.* 1998; Wolska *et al.* 1999). Results from β-TM TG mouse studies show that TG myocardium expressing β-TM protein exhibits decreased maximum rate of relaxation in the isolated heart preparations (Muthuchamy *et al.* 1995), increased calcium sensitivity in skinned fibre preparations (Palmiter *et al.* 1996), and both decreased maximal rates of contraction and relaxation in isolated cardiomyocytes (Wolska *et al.* 1999). We initially hypothesized that the two charge modifications in β-TM, Ser229Glu and His276Asn, are responsible for these altered contractile parameters. To test this, we have recently created a mutant form of murine striated α-TM that contains a charge change in both of these regions: α-TM Ser229Glu + His276Asn or α-TM DM for double mutation (Gaffin *et al.* 2004). Results showed that both $+\mathrm{d}P/\mathrm{d}t$ and $-\mathrm{d}P/\mathrm{d}t$ decreased in isolated working hearts, and calcium sensitivity decreased in skinned fibre preparations (Gaffin *et al.* 2004). These two charge residue changes occur in unique regions of α-TM. The Ser229Glu change occurs in the inner core region of TM molecule, residues 143–235, that is considered to be less stable than other regions of the molecule (Paulucci *et al.* 2002). The His276Asn change occurs in the carboxyl terminal overlap region of the molecule, which is essential for it to interact with TnT and contiguous TMs in a head-to-tail fashion. Since these two charge change residues are found in diverse regions of TM, we hypothesized that individually mutating these charged residues on α-TM would affect cardiac function differently.

To test this hypothesis, in this study we have generated two different TG lines, α-TMSer229Glu and α-TMHis276Asn, which contain charge change mutations at positions 229 and 276, respectively. Results show that α-TM229 transgenic (TG) hearts exhibit a decrease in both $+\mathrm{d}P/\mathrm{d}t$ and $-\mathrm{d}P/\mathrm{d}t$ in isolated working heart preparations, a decrease in calcium sensitivity in skinned fibre preparations, and give indications of a decrease in calcium sensitivity and an increase in strong crossbridge formation in intact papillary fibres. α-TM276 mouse hearts exhibit a decrease only in $-\mathrm{d}P/\mathrm{d}t$ in the isolated working heart and no change in calcium sensitivity in skinned fibres, but give indications of an increase in both calcium sensitivity and strong crossbridge formation in intact papillary fibres when compared to nontransgenic (NTG) fibres. Thus, our data provide the first evidence that charge changes at various regions of TM affect cardiac performance differently.

Methods

Generation of the TG mice

Site-directed mutagenesis was used to generate mutations in α-TM cDNA at codon 229, TCT to GAG (α-TM229), and codon 276, CAC to AAC (α-TM276). The α-TM mutant cDNAs were then ligated to clone 26 which contains the cardiac-specific α-myosin heavy chain (MHC) promoter (Subramaniam *et al.* 1991) and the human growth hormone (HGH) poly(A) signal sequence. Mutations were verified by sequencing. The procedures for FVB/N TG mice generation have been described. (Gaffin *et al.* 2004) Briefly, *Bam*HI enzyme was used to release the transgene fragment (7.2 kb) from the pBluescript II vector. The transgene was purified using electroelution and the purified DNA was microinjected into male pronuclei for founder mouse generation. These were identified using PCR as described (Walter *et al.* 1989). PCR primers corresponding to nucleotide sequences within the second intron of the MHC promoter and the α-TM cDNA were annealed to genomic DNA from ear clips producing a 234 bp fragment in TG mouse tissue. Stable transgenic lines were raised by breeding the founder TG mice with NTG cohorts. All experiments using mouse hearts were approved by the Texas A and M University Animal Care Committee.

S1 nuclease mapping

Total RNA was isolated from both NTG and TG mouse hearts using RNA-Stat 60 (Tel.Test, Friendswood, TX, USA). Quantification of endogenous *versus* TG transcripts were performed by using S1 nuclease protection assay as described (Gaffin *et al.* 2004). Briefly, to distinguish α-TM229 and α-TM276 transcripts from endogenous α-TM mRNAs, a PCR probe that incorporates the second and third exon of α-MHC (15 bp) and 262 nucleotides of the α-TM coding region was utilized. In S1 nuclease mapping analyses, this probe protects 262 nucleotides of endogenous α-TM, whereas a 277 bp fragment is protected for mutant α-TM transcripts. A control glyceraldehyde-3-phosphate dehydrogenase (GAPDH) probe was used for quantitative purposes.

DNA probes for the hybridization reaction were created using PCR. Single-stranded DNA probes used for hybridization were labelled at the 3′-end with γ-^{32}P adenosine triphosphate (Amersham) via T4 kinase (Invitrogen). The sequences for the S1 probes were as follows: 5′-TM primer, 5′-GCCCACAC-CAGAAATGACAGACAG-3′; 3′-TM primer, 5′-GAGA-AGCTACGTCAGCTTCAGCAT-3′; GAPDH probe was also prepared via PCR. Hybridized RNA–DNA strands were electrophoresed on 6% polyacrylamide gels (19 : 1) containing 8.3 M urea. Gels were dried and auto-radiographed on Kodak X-Omat AR film. Densitometry analysis of the resulting bands using Multi-Analyst software and phosphorimaging analyses were conducted to determine RNA content. Quantification was performed using the volume integration method with subtraction of the tRNA control lane as background. Three separate RNA gels were used to quantify the relative levels of transcripts.

Gel electrophoresis and Western blotting

Modified procedures from Pagani & Solaro (1984) were used to isolate myofibrils from the heart with all solutions being supplemented with 1 μg μl^{-1} leupeptin and 1 mM phenylmethylsulphonyl fluoride; 7.5 μg protein was separated on a 10% SDS gel containing 3.4 M urea (Schachat *et al.* 1985) and transferred to a nitrocellulose membrane for Western blot analysis. Primary antibody incubations were performed with a striated muscle-specific TM antibody, CH-1 (Developmental Studies Hybridoma Bank, University of Iowa) that recognizes both endogenous and mutant forms of TM. Secondary antibody incubations were performed with goat-antimouse IgG conjugated to horseradish peroxidase (Sigma). Chemiluminescence (SuperSignal West Pico; Pierce) was used as the detection agent. Densitometry on the resulting bands was performed using Multi-Analyst software. To verify equal loading of each sample, membranes were stripped using Immuno-Pure IgG Elution Buffer (Pierce) and then reprobed with antisarcomeric actin antibody (Sigma). The resulting TM/actin ratio was used as an indicator of equal loading. Western blot analysis of myofibrillar proteins followed by quantification was performed three times for each sample and the resulting mean values ± S.E.M. calculated.

Two-dimensional gel electrophoresis

Two-dimensional gel electrophoresis was performed according to the method of O'Farrell (1975). Briefly, myofibrillar proteins from mouse hearts were prepared as outlined above; however, the concluding washes after Triton X-100 treatment were conducted in the following low-salt solution: (mM) 20 KCl, 2 KH_2PO_4, 2 ethylene glycol-bis[β-aminoethyl ether]-*N*,*N*,*N*′,*N*′-tetraacetic acid (EGTA), and 0.5 mM phenylmethylsulfluoride (PMSF); 25 μg of protein in this protein suspension was then dissolved and reduced in 300 μl of isoelectric focusing sample (rehydration) buffer (8 M deionized urea, 2% 3-[(3-cholamidopropyl)dimethylammonio]-1-propanesulphonate (CHAPS), 2 mM tributylphosphine, and 0.2% Bio-Lytes (4.7–5.9; Bio-Rad)). Each protein sample was then used to rehydrate a 17 cm ReadyStrip (pH 4.7–5.9; Bio-Rad) for 16 h. Isoelectric focusing was then performed in three stages, utilizing the following voltage protocol: 250 V for 15 min (rapid ramp); 10 000 V for 1 h (slow ramp); 8000 V for 40 000 V h (rapid ramp). Focused strips were then treated with equilibration buffer (6 M urea, 2% sodium dodecyl sulphate (SDS), 0.375 M Tris-HCl pH 8.8, 20% glycerol) containing 2% dithiothreitol (10 min), followed by treatment with equilibration buffer containing 2.5% iodoacetamide (10 min treatment). The strips were then applied to 15% acrylamide gels for SDS-PAGE, followed by transblotting onto nitrocellulose membranes. Western blot analysis was similar to that described above except CH-1 antibody was used in a 1 : 15 000 dilution and secondary antibody was used in a 1 : 30 000 dilution.

Physiological measurements of left ventricular function

The isolated working heart preparations have been described (Gulick *et al.* 1997). Age- and sex-matched mice (4–6 months) were used in this study. Female α-TM276 TG mice were compared to female NTGs in these experiments due to difficulties obtaining a sufficient number of male α-TM276 TG mice. Briefly, mice were deeply anaesthetized with sodium pentobarbital (150 mg (kg body weight)$^{-1}$ I.M.), and the hearts were immediately excised. A 20-gauge cannula was tied onto the aortic stump to allow regulation and recording of mean arterial pressure (MAP) and aortic flow (Transonic Flow Probe Model T206; Transonic Systems Inc., Ithaca, NY, USA). A silastic fluid-filled catheter was inserted through the apex of the left ventricle to record intraventricular pressure. Left ventricular pressure was measured as systolic, diastolic, and end-diastolic pressure using the DigiMed Systems Analysers BPA-2000, HPA-200, HPA-210, and LPA-200 (Micro-Medical, Inc., Louisville, KY, USA). The fluid-filled catheter system responded well within experimental requirements without distortion, up to a frequency of 600 bpm. A 20-gauge cannula was tied into the left pulmonary vein to accommodate regulation on recording of venous return (cardiac output). The catheter was completely water-jacketed for improved temperature (37.4°C) regulation of the Krebs–Henseleit solution (mM: 119.0 NaCl, 11.0 glucose, 4.6 KCl, 25.0 $NaHCO_3$, 1.2 KH_2PO_4, 1.2 $MgSO_4$, and 1.8 $CaCl_2$) that was returned to the left side of the heart for anterograde perfusion. Custom-designed software calculated heart rate, MAP, left ventricular pressure, peak systolic pressure, time to peak pressure (TPP), half time of relaxation, the first derivatives of the change in left ventricular systolic pressure with respect to time ($\pm dP/dt$), left atrial pressure, and perfusate temperature. The arterial P_{O_2} was 650 mmHg and the P_{CO_2} −30 mmHg. The data are expressed as mean ± S.E.M. Starling curves were generated by linear regression using Statview version 5.0.1 (Abacus Concepts Inc., Berkeley, CA, USA).

Skinned fibre force–Ca^{2+} measurements

Force–calcium relationships using skinned fibre preparations of left ventricular papillary fibres have been described (Gaffin *et al.* 2004). In brief, adult mice (3–4 months old; 25–35 g) were anaesthetized with sodium pentobarbital (150 mg (kg body weight)$^{-1}$ I.M.), and the hearts quickly removed and put into high-relaxing solution of the following composition (mM): 53.3 KCl, 10

EGTA, 20 MOPS, 1 free $MgCl_2$, 5.4 MgATP, 12 creatine phosphate. The pH of the solution was adjusted to 7.0 with KOH. Papillary muscles from the left ventricle were dissected, and small fibre bundles ~150–250 μm in width and 2–3 mm in length were prepared. The fibre bundles were mounted between clips on a micromanipulator and a force transducer. Fibres were skinned for 30 min in high-relaxing solution containing 1% Triton X-100. After skinning, the fibres were initially washed with high-relaxing solution and then sequentially bathed in low-relaxing solution. Compared to high-relaxing solution, low-relaxing solution contains 0.1 mM EGTA. A resting sarcomere length of 2.2 μm was then established from laser diffraction patterns (Hibberd & Jewell, 1982). Isometric tension was recorded on a digital phosphor oscilloscope suite (Tektronix TDS 3014 with Wavestar software) after development in solutions of varying pCa^{2+} values. After initial Ca^{2+}–force relationships were established, cAMP-dependent phosphorylation of skinned fibres was induced by incubation in low-relaxing solution containing 100 μM cAMP + 100 ng ml^{-1} calyculin A, for 30 min (Palmiter *et al.* 1996). Force development was again recorded using similar solutions with the addition of 100 μM cAMP + 100 ng ml^{-1} calyculin A. Results are presented as mean ± S.E.M. The force–pCa relation was fitted to the Hill equation with nonlinear analysis to derive the pCa_{50} and Hill coefficient using Prism software. Shifts in the pCa_{50} value and the Hill coefficient were analysed using an unpaired Student's *t*-test, with significance set at $P < 0.05$.

Force–frequency with calcium measurements in intact papillary muscle fibres

Right ventricular papillary muscles were dissected from FVB/N mouse (4–5 months) hearts in 4°C Krebs–Henseleit (KH) solution containing 20 mM 2,3-butadione monoxime (BDM). The KH solution consisted of (mM) 119.0 NaCl, 11.0 glucose, 4.6 KCl, 25.0 $NaHCO_3$, 1.2 KH_2PO_4, 1.2 $MgSO_4$, and 1.8 $CaCl_2$. The KH solution was equilibrated to a pH of 7.4 with 95% O_2 and 5% CO_2. Incisions were made on the valve, and a wide ventricular region around the base of the bundle so as not to damage the fibre. The muscle approximates a two-dimensional triangle as it tapers from the right ventricular wall towards the tricuspid valve with the width of the base being ~0.45–0.6 mm, the depth at the base being 0.2–0.3 mm, and the length of the triangle being 0.6–1.2 mm. The force was normalized to cross-sectional area at the base using approximate cross-sectional area = 0.75 × width × depth (Li *et al.* 2000). All experiments were carried out at 21°C.

The intact bundles plus chordae tendinae were mounted at the valve and the ventricular region by clips between a force transducer and a voltage-controlled motor positioner within a muscle measurement suite (Scientific Instruments, Germany). Stimulation pulse duration was 3.5 ms with an initial rate of 0.5 Hz. The papillary bundle was continuously superfused with KH maintained at room temperature. Stimulation voltage and bundle length were adjusted until maximum force was reached. The fibre bundle was then stimulated at 0.5 Hz for 45 min before executing the experimental protocol. A digital phosphor oscilloscope suite (Tektronix TDS 3014 with IEEE-488 communication module and Wavestar™ software) measured stimulation frequency, twitch force amplitude, averaged force amplitude within preset time windows, and continuously logged the data into the computer.

The same muscle measurement equipment suite provided all the optics and electronics needed for measuring intracellular calcium with Fura-2 dye. Measurements, however, were collected through a different data acquisition suite (National Instruments A/D board and Labview software) with the digital oscilloscope suite providing continuous monitoring. A mercury lamp and filter-wheel provided alternating ultraviolet (UV) pulses of 340 nm and 380 nm at 250 Hz with pulse duration of 1.5 ms to illuminate the bundle. A combination of microscope, dichroic mirror, filter, and photomultiplier tube (PMT) collected the Fura-2 fluorescence. The loading solution consisted of KH with 10 μM Fura-2-AM dissolved in dimethyl sulfoxide (DMSO; KH : DMSO was 333 : 1) and 5.0 g l^{-1} cremophor to increase loading efficiency. A loading duration of 1.5 h gave signals of greater than three-fold over background fluorescence. The ratio, *R*, of fluorescence (emission at 510 nm) from 340 nm excitation to fluorescence from 380 nm excitation was calculated after subtracting background fluorescence. Calcium concentration was then calculated using the equation below (Grynkiewicz *et al.* 1985) after an *in vitro* calibration with 10 μM Fura-2 pentapotassium salt (Initially we used Fura-2-AM to obtain the R_{min} and R_{max} values. In these experiments we have to use ionophores (e.g. ionomycin). There were two problems: (1) variations in the effects of ionophores from experiment to experiment; (2) inconsistent values of R_{max} for each experiment. This led to huge differences in the calculation of intracellular calcium concentrations from experiment to experiment. On the other hand, *in vitro* calibration with the known calcium solution using Fura-2 salt simulated *in vivo* conditions and yielded consistent R_{min} and R_{max} values that were used for calculating the calcium concentrations, which were comparable from experiment to experiment).

$$[Ca^{2+}]_{IC} = k_d \beta (R - R_{min}/R_{max} - R) \qquad (1)$$

Values for the equations were as follows: k_d, 283 nM, as taken from Backx & Ter Keurs (1993); β, 9.96 (calculated as the ratio of fluorescence from 380 nm excitation at zero calcium to 380 nm excitation at saturating calcium); R_{min},

0.13, and R_{max}, 3.16. R_{max} is defined as the 340 : 380 at saturating calcium (10 mM Ca^{2+}) while R_{min} is the 340 : 380 in the absence of calcium (0 mM Ca^{2+} + 10 mM EGTA).

Data analyses of the force–calcium loop

Data analyses were done as we have recently described (Tong *et al.* 2004). Briefly, to analyse the force–calcium loop, we first measured calcium and force values at specific points during a contraction cycle consisting of: (1) the resting point, 'A' (2) the maximum calcium point, 'B', and (3) the maximum force point, 'C'. These three points provide a snapshot of pivotal transitional states of the force–calcium loop. However, analyses of the data, with regard to changes in force and calcium concentrations, were performed only at points B and C, as described in the results section. We also analysed segments of the force-calcium loop using two different equations that describe the C to A and B to C segments (Tong *et al.* 2004).

Equation (2) is the Hill equation. It fits well with data points from the C to A segment.

$$\text{Force} = F_0\left([Ca^{2+}]_{IC}{}^n / k_d{}^n + [Ca^{2+}]_{IC}{}^n\right) + \text{offset} \qquad (2)$$

Here, F_0 is the maximum active force and k_d is the $[Ca^{2+}]_{IC}$ at 50% maximum active force in the relaxation segment of the force-calcium loop. The parameter n represents the slope of the line as it does in the Hill equation, and offset is defined as the force associated with point A (optimal preload).

Equation (3) is a modified reciprocal of the Hill equation that fits well with data points from the B to C segment. It is based largely on empirical fit.

$$\text{Force} = G k_d{}^n / \left(k_d{}^n + [Ca^{2+}]_{IC}{}^n\right) + \text{offset} \qquad (3)$$

Here G represents the maximum active force attained within this segment (point C), and k_d could be an indicator of strong crossbridge activation since it occurs in the portion of the force–calcium loop where the majority of force is developed. Again, the parameter 'n' represents the slope of the B–C segment, and offset is defined as the force associated with point B.

Statistical analyses

All data are expressed as mean ± S.E.M. Statistical analyses were done using an analysis of variance (ANOVA) with Fisher's *post hoc* test or a two-way ANOVA with Bonferroni/Dunn's *post hoc* test, as appropriate. In addition, linear regression and analysis of covariance (ANCOVA) analyses were done for the working heart data. $P = 0.05$ was regarded as statistically significant.

Results

Generation and molecular characterization of TG mice

α-TM cDNA was used in site-directed mutagenesis to generate two different constructs: α-TM229 and α-TM276 (Fig. 1*A*). Constructs were isolated from the vector DNA using *Bam*H1 enzyme, purified via electrophoresis, and injected into male pronuclei to produce founder TG mice. Germ-line transmission of the transgene was confirmed by PCR analysis of DNA from mice ear clips. Southern blot analysis was also conducted to verify the presence of the 7.2 kb transgene within the genomic DNA of TG mice (data not shown). None of the founder mice or their progeny from either mutation demonstrated any gross phenotypic alterations or reduced viability.

TG expression at the mRNA level was determined in TG mouse hearts using the S1 nuclease protection assay (Gaffin *et al.* 2004). A band corresponding to mutant α-TM (277 nt) can be seen in all TG heart RNA samples (Figs 1*B* and *C*). In the face of significant expression of the transgenically encoded TM species, endogenous TM RNA levels were downregulated in all TG lines except α-TM276 line 6. Quantitative phosphorimaging and densitometry analyses show that 94.7% mutant α-TM229 message is present in TG line 229-4. 229-22, 229-24, and 229-D TG lines have 86.7%, 95.5% and 93.6% mutant transcripts, respectively. Furthermore, 94.7% of the total TM transcript pool is transgenically encoded in TG line 276-5. Line 276-6 has 57.4% mutant transcripts. Note that the total level of TM transcripts is significantly higher in line 276-6 when compared to the total NTG TM levels.

To examine the effects of α-TM mutant transgene expression on the myofilament protein profile, we analysed myofibrillar protein fractions of both TG and NTG hearts. Initial experiments using SDS-PAGE could not resolve endogenous from mutant α-TM protein in both TG lines (data not shown). However, α-TM229 mutant protein was able to be separated from endogenous α-TM in SDS-PAGE gels containing 3.4 M urea (Schachat *et al.* 1985). Unfortunately, α-TM276 mutant protein was still not resolvable in urea gels. To confirm the presence of mutant α-TM protein bands in α-TM229, Western blot analyses were carried out. Figure 2*A* shows that NTG samples contain only one band while TG samples contain two bands, the slower migrating α-TM229 and the endogenous TM band. Quantification analyses demonstrate that line 229-4 expresses higher levels of mutant protein (98.4%) compared with that of 229-22 (86.7%), 229-24 (95.5%), and 229-D (93.6%) (Fig. 2*B*). These protein results corroborate well with the RNA data.

In order to resolve α-TM276 mutant band from the endogenous α-TM band, two-dimensional gels were utilized (Fig. 3). Note that the α-TM protein spot from NTG heart (Fig. 3*A*) sample falls near its pI value of 5.1 as we have shown in our previous studies (Muthuchamy

et al. 1995) and that the TG α-TM276 samples resolved into two spots (Fig. 3*B* and *C*). The spot in the position of pI value of 5.1 is the endogenous TM, and the mutant protein spot shifts towards a more acidic pI (i.e. closer to 4.7) due to the loss of a basic residue at amino acid 276. Quantitative determination revealed that 82.4% and 40.2% of mutant TM protein is present in the TG α-TM276-5 and α-TM276-6 hearts, respectively.

α-TM229 and 276 differentially affect cardiac function

In order to determine the functional properties of charge changes in α-TM mutant hearts, isolated cardiac function in the absence of neurohumoral input was assessed using work-performing isolated heart preparations in age- and sex-matched NTG and α-TM TG mutant hearts. We used the TG lines with the highest levels of mutant TM protein expression in all physiological analyses (i.e. line 4 for TG α-TM229 mice and line 5 for TG α-TM276 mice). Figure 4*A* shows an example of various contractile parameter tracings from a NTG heart that was used for analyses. The α-TM229 hearts are hypodynamic as evidenced by their attenuated rates of contraction ($+dP/dt$) and rates of relaxation ($-dP/dt$) (Table 1). Furthermore, TPP is changed in the α-TM229 TG

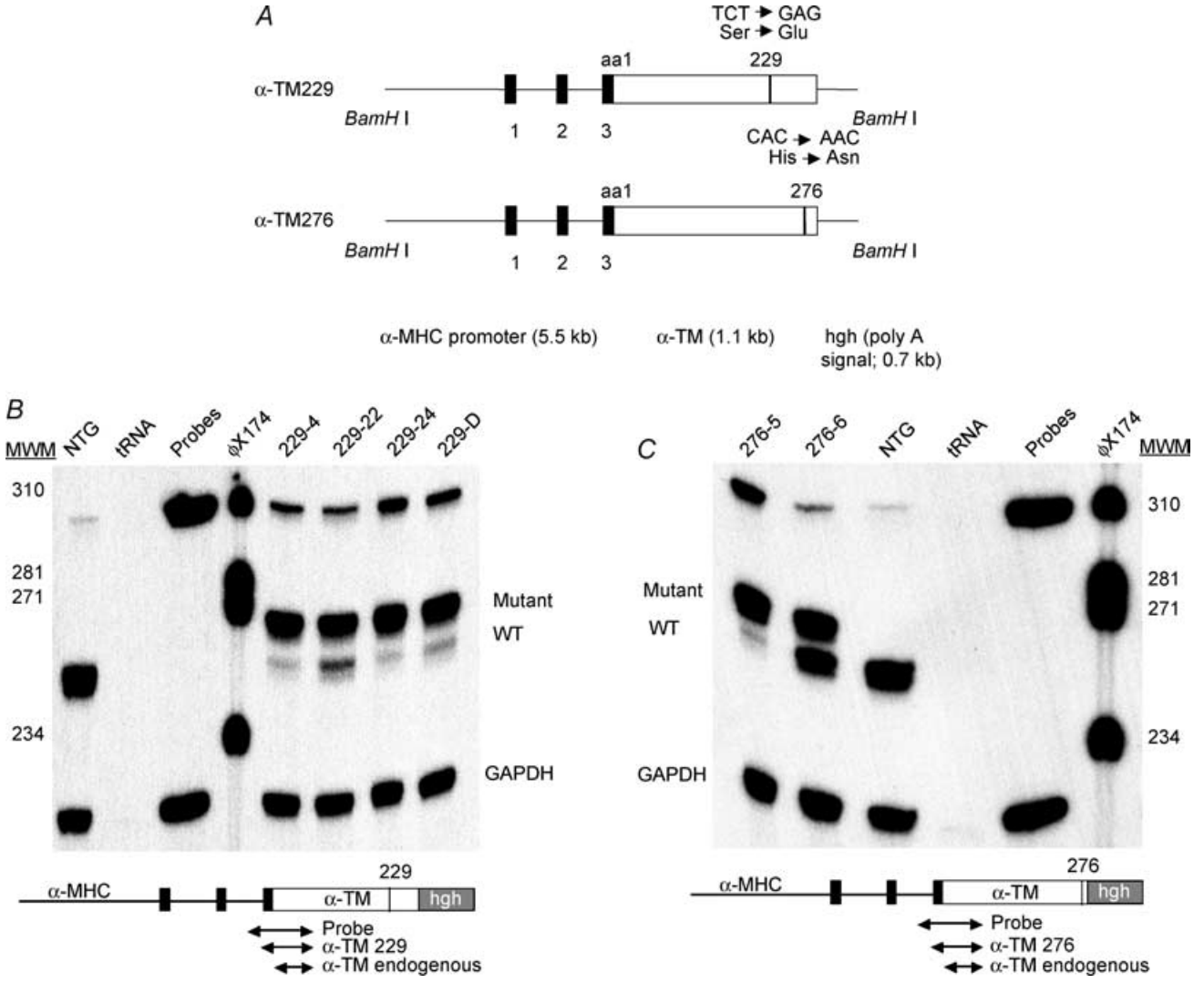

Figure 1. TG constructs and mRNA expression

A, schematic representation of the TG constructs. Mutant TM cDNAs (either Ser229Glu or His276Asn) were linked to the α–MHC promoter and used to generate multiple lines of TG mice (Subramaniam *et al.* 1991). The human growth hormone polyadenylation site (hgh poly A) was placed downstream of either TM cDNA. The black boxes denote the α–MHC exons that encode the 5′-untranslated region. The construct was released using *Bam*HI enzyme. B and C, RNA expression in α-TM229 and α-TM276 TG mice, respectively; 20 μg of total cardiac RNA was hybridized to 3′-radioactively labelled DNA probes specific for either TM (see the small diagram below the RNA gel) or GAPDH. TM probe is 320 bp in length and yields fragments of 277 bp for mutant and 262 bp for endogenous TM RNA after S1 nuclease treatment. The electrophoresed samples shown here contain both mutant and endogenous bands for α-TM229 samples and an endogenous band only for NTG hearts. tRNA was used as a negative control.

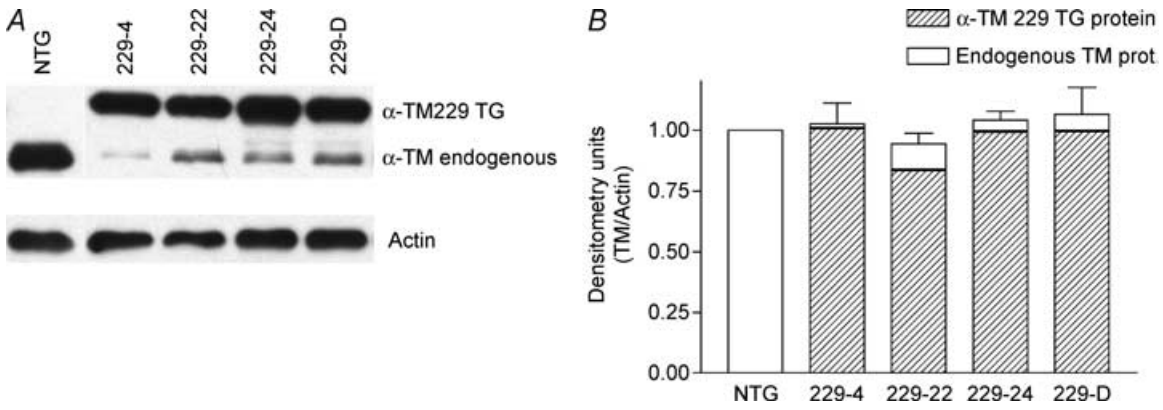

Figure 2. Protein expression in TG α-TM229 mice
A, Western blot of total α-TM229 myofibrillar proteins electrophoresed on SDS-PAGE gels containing 3.4 M urea. Nitrocellulose filters were first probed with a striated muscle-specific TM antibody, CH-1, then stripped and reprobed with a sarcomeric actin-specific antibody to verify equal loading for each sample. *B*, densitometry analysis of Western blots shown in *A*. The relative levels of mutant protein expression were quantified (Gaffin *et al.* 2004) and in each sample, total α-TM229 plus endogenous TM was divided by the actin and the data compared to the NTG levels. Total TM levels were similar for NTG and TG samples. Results were obtained from three different experiments and data are presented as mean ± S.E.M.

hearts. α-TM276 hearts exhibit a significant decrease in the relaxation rate, and the rate of contraction is also decreased, albeit nonsignificantly ($P = 0.07$) (Table 1). In addition, the ratio of dP/dt maximum : minimum is significantly increased in α-TM276 TG hearts, indicating impaired relaxation. In addition other contractile and relaxation parameters such as TPP and τ are also significantly altered in α-TM276 hearts. Thus, the data show that the cardiac performance of these TG hearts is significantly affected by charge changes in α-TM.

Figures 4*B* and *C* show the Frank–Starling left ventricular functional curves for NTG and α-TM229, and NTG and α-TM276 TG groups, respectively. The plots of cardiac work *versus* the rates of pressure development and relaxation indicate a positive correlation for both NTG and TG hearts. In addition, the slopes calculated by linear regression analyses are not significantly changed in the TG groups compared to NTG (see Fig. 4 legend). However the slope of the relationship between +dP/dt and cardiac work in α-TM229 hearts is reduced (9.64 for control hearts *versus* 7.63 for α-TM229) albeit nonsignificantly ($P = 0.06$). As shown in Table 1, +dP/dt and −dP/dt are significantly reduced in α-TM229 hearts, and −dP/dt is reduced in α-TM276 hearts as analysed by ANCOVA. Furthermore, as seen in Fig. 4*C*, α-TM276 hearts do not function well at a higher workload that is correlated well with the decrease in left ventricular pressure in these TG hearts (Table 1).

α-TM229 and 276 have differential effects on myofilament calcium sensitivity

To further determine the mechanisms for altered rates of contraction and relaxation in the α-TM TG mouse hearts, we measured isometric force in myofilaments prepared from NTG and α-TM mutant mouse hearts. Force generated by TG α-TM229 myofilaments was significantly less sensitive to Ca^{2+} when compared with NTG myofilaments (Fig. 5*A*). The pCa_{50} for NTG preparations is 5.83 ± 0.02 and 5.73 ± 0.02 for α-TM229 myofilament preparations ($n = 8$ from four different hearts; $P = 0.01$). However, the pCa_{50} for α-TM276 TG myofilaments was not significantly different from NTG myofilaments (5.81 ± 0.04; $n = 8$ from four different mice; Fig. 5*C*). In addition, neither mutation in α-TM demonstrated a significant change in cooperativity. The Hill coefficient was 3.40 ± 0.18 for NTG, 3.64 ± 0.24 for α-TM229, and 3.62 ± 0.25 for α-TM276 fibres.

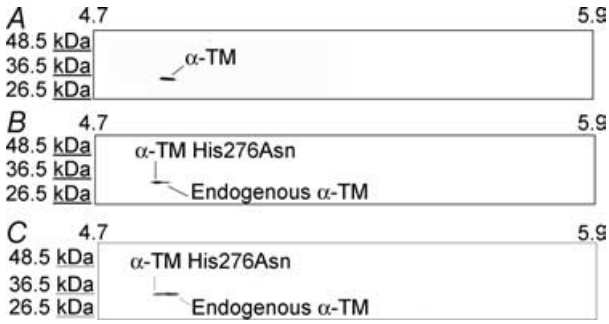

Figure 3. Two-dimensional gel analyses of NTG and TG α-TM276 myofibrillar proteins
Total myofibrillar proteins from both NTG (*A*) and TG α-TM276 (*B* and *C*, line 5 and 6, respectively) hearts were subjected to reduced-reduced two-dimensional electrophoresis and transferred to nitrocellulose membranes, which were then probed with a striated muscle-specific TM antibody, CH-1. pI values (4.7–5.9) are indicated at the top. The TG samples contain both α-TM276 and endogenous TM spots while the NTG sample contains only endogenous α-TM.

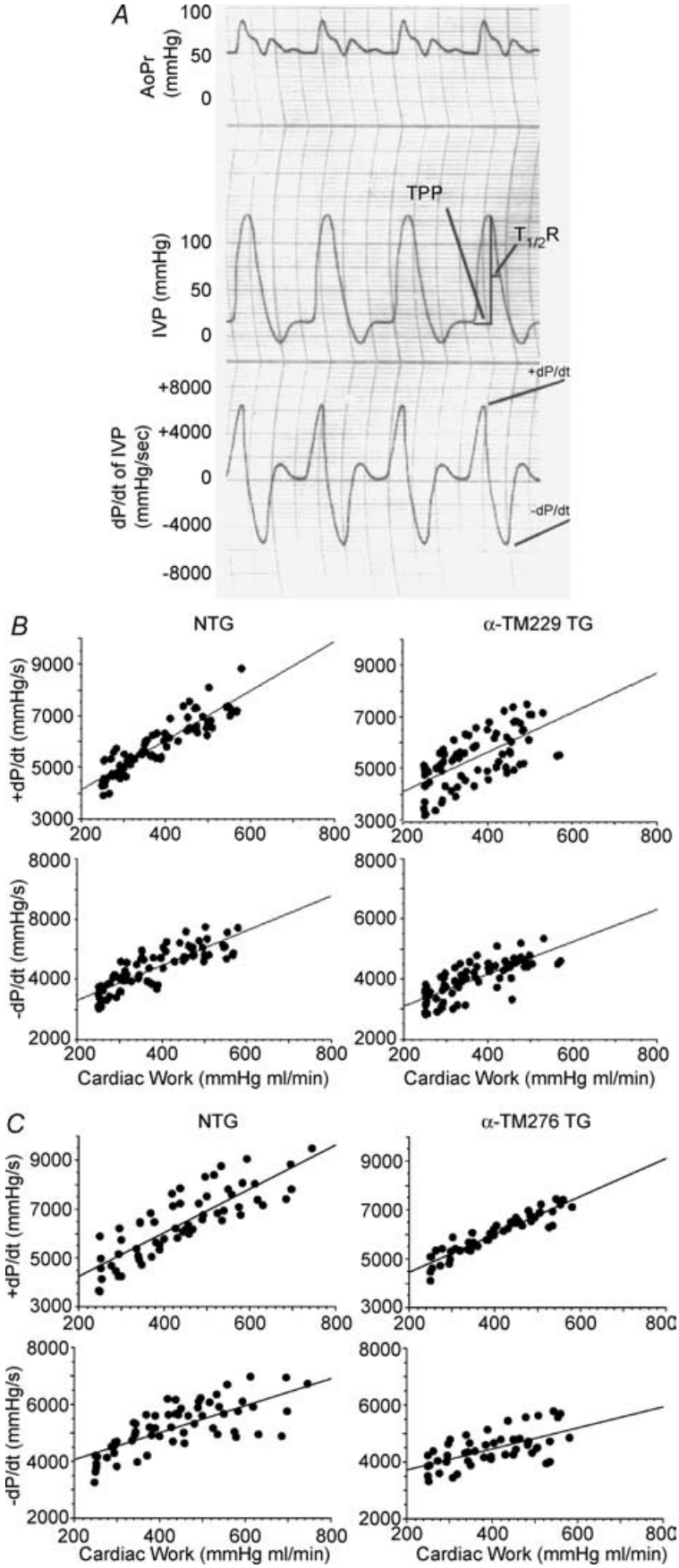

Figure 4. Frank-Straling left ventricular functional curves

A, contractile measurements tracing of representative isolated mouse heart preparation from NTG female mouse. Time to peak pressure (TPP) and time to 50% relaxation ($T_{1/2\,R}$) are marked on the tracing. IVP: intraventricular pressure, AoPr: aortic pressure. *B* and *C*, responses of isolated working hearts to different range of workloads.The derivatives of pressure parameters, $+dP/dt$ and $-dP/dt$ were plotted against a continuum increase workload for both NTG and α-TM229 and α-TM276 experimental groups. The linear regression analyses yielded the following regression lines for NTG and TG groups (W, work; Y, $\pm dP/dt$):

NTG hearts	$+dP/dt$	$Y = 2190.531 + 9.635W$
α-TM229 TG hearts	$+dP/dt$	$Y = 2569.621 + 7.633W$
NTG hearts	$-dP/dt$	$Y = 2164.618 + 5.783W$
α-TM229 TG hearts	$-dP/dt$	$Y = 2025.222 + 5.377W$
NTG hearts	$+dP/dt$	$Y = 2457.18 + 8.97W$
α-TM276 TG hearts	$+dP/dt$	$Y = 2901.89 + 7.76W$
NTG hearts	$-dP/dt$	$Y = 3121.62 + 4.74W$
α-TM276 TG hearts	$-dP/dt$	$Y = 2980.27 + 3.69W$

Table 1. Contractile parameters of NTG, TG α-TM229 and TG α-TM276 mouse hearts

Working hearts	NTG male hearts ($n = 8, 80$)	α-TM229-4 male hearts ($n = 8, 80$)	% change *versus* NTG males	NTG female hearts ($n = 6, 60$)	α-TM276-5 female hearts ($n = 5, 50$)	% change *versus* NTG females
Heart rate (bpm)	407 ± 1	402 ± 1	Paced*	405 ± 1	408 ± 2	Paced**
$+$dP/dt (mmHg s^{-1})	5828 ± 119	5392 ± 117	-7*	6398 ± 180	6000 ± 116	N.S. (0.07)
$-$dP/dt (mmHg s^{-1})	4348 ± 77	4013 ± 70	-8*	5203 ± 110	4452 ± 84	-14***
$+$dP/dt/$-$dP/dt	1.34 ± 0.03	1.34 ± 0.02	N.S.	1.22 ± 0.02	1.35 ± 0.02	$+11$***
LVP (mmHg)	105 ± 2	103 ± 2	N.S.	116 ± 2	101 ± 2	-13***
ED LVP (mmHg)	7.2 ± 1	8.1 ± 1	N.S.	6.0 ± 1	5.1 ± 1	N.S.
TPP (ms)	52 ± 1	45 ± 1	-13***	46 ± 1	51 ± 1	$+11$***
Time to 1/2R (ms)	33 ± 1	32 ± 1	N.S.	33 ± 1	33 ± 1	N.S.
τ (ms)	25 ± 1	25 ± 1	N.S.	17 ± 1	21 ± 1	$+24$***

*$P = 0.05$, **$P = 0.01$,***$P = 0.001$, control *versus* transgenic or transgenic *versus* transgenic, ANOVA Values are means $\pm$ S.E.M. S.E.M. = standard error of the mean; LVP = peak systolic left ventricular pressure. ED LVP = end diastolic left ventricular pressure; TPP = time to peak pressure; time to 1/2R = time to 50% relaxation; τ = the time constant in milliseconds of the best-fit exponential pressure decay from the pressure at maximum negative dP/dt to a positive pressure above the previous ventricular end diastolic pressure by 10 mmHg; N.S. = not significant.

In order to assess the effect of TnI phosphorylation on calcium sensitivity in α-TM mutant TG mice, we incubated skinned fibre bundles with 100 μM cAMP and 100 ng ml^{-1} calyculin A, a phosphatase inhibitor. This treatment mimics the effects of β_1 adrenergic stimulation, which causes a characteristic decrease in calcium sensitivity upon phosphorylation of TnI by PKA (Guo *et al.* 1994; Palmiter *et al.* 1996). Our results in NTG fibres yielded a pCa_{50} of 5.83 ± 0.02 before cAMP treatment and 5.75 ± 0.01 after cAMP treatment ($n = 8$ from four different NTG hearts). Fibre bundles from both α-TM charge change mutations also displayed a rightward shift in calcium sensitivity. The average difference in pCa_{50} between cAMP-treated and -untreated fibres for both mutations was between 0.08 and 0.11 pCa units (Fig. 5*B* and *D*), which is similar to the shift seen in NTG fibres. In addition, neither mutation exhibited a significant change in cooperativity. These findings were confirmed in adrenergic dose-dependent responses from working heart preparations of α-TM229 mice, which displayed increases in $-$dP/dt similar to NTGs upon addition of isoproterenol (data not shown). Thus, the decrease in Ca^{2+} sensitivity in response to TnI phosphorylation is maintained in the TG preparations when compared with NTG samples.

Thin filament activation mechanisms are altered in TG fibres

To further assess thin filament activation mechanisms in these TG models, we simultaneously measured force and intracellular calcium ($[Ca^{2+}]_{IC}$) in isolated, intact papillary fibres. This method is a more sensitive means of assessing calcium sensitivity since k_D and cooperativity values are higher in intact fibres *versus* skinned fibres (Gao *et al.* 1994). Possible reasons for these discrepancies are described by Gao *et al.* (1994). Furthermore, we have recently described the components of the force–calcium loop and have discussed that both calcium activation of the thin filament and positive feedback by strongly bound crossbridges contribute significantly to each phase of the contractile cycle (Tong *et al.* 2004). Thus, alterations in myofilament activation mechanisms can be determined by analysing the force–calcium data.

Traces from single NTG, α-TM229 and α-TM276 fibres show that both force and $[Ca^{2+}]_{IC}$ increase with increases in stimulation frequency (Fig. 6*A*). At all stimulation frequencies, force relates to calcium concentration in a hysteresis loop fashion. In addition, increasing the stimulation frequency causes both increased calcium transients ($\Delta[Ca^{2+}]_{IC}$), and increased active force. The force–calcium loop can be considered to start after full relaxation from a contraction and is labelled 'A' on the calcium-force cycle (Fig. 6*B*). Point B represents maximum calcium concentration and point C represents maximum force production.

In order to analyse the force–calcium traces, we chose two methods of analyses. The first method focuses on the points of minimal force/calcium (A; see Fig. 6*B*), maximal $[Ca^{2+}]_{IC}$ (B), and maximal force (C). At point A, force is merely passive tension (usually between 3 and 5 mN mm^{-2}) and the $[Ca^{2+}]_{IC}$ associated with it; thus, point A does not portray any active work generated by the fibre and was not used in the analysis. Fig. 7*A*–*C* shows the maximum $[Ca^{2+}]_{IC}$, maximum active force, and maximum active force divided by the change in $[Ca^{2+}]_{IC}$ (force/$[Ca^{2+}]_{IC}$) for each of the four stimulation frequencies: 0.5 Hz, 1 Hz, 2 Hz, and 3 Hz, respectively. Force/$[Ca^{2+}]_{IC}$ is defined as the active force divided by the difference in $[Ca^{2+}]_{IC}$ between points A and C. This parameter describes the amount of active force produced

by the fibre, normalized to the change in $[Ca^{2+}]_{IC}$; thus, it is an indirect assessment of myofilament calcium sensitivity at this point in the force–calcium loop. In α-TM229, maximum $[Ca^{2+}]_{IC}$ does not appear to be different from that seen in NTGs although statistical significance occurs over the range of frequencies studied ($P = 0.047$), probably due to the extremely small variability seen in NTGs for 0.5 and 1 Hz (Fig. 7*A*). Maximum active force is not statistically significant ($P = 0.108$) over the range of frequencies studied, although force seems to decrease at the higher frequencies (Fig. 7*B*). The calcium sensitivity parameter, force/$[Ca^{2+}]_{IC}$, decreases dramatically, which indicates that α-TM229 myofilaments are less sensitive to calcium (Fig. 7*C*). In α-TM276, $[Ca^{2+}]_{IC}$ decreases while active force remains the same as in NTG fibres, which causes an increase in force/$[Ca^{2+}]_{IC}$ ($P = 0.054$). Thus, α-TM276 fibres display an increase in calcium sensitivity at the point of maximum force generation.

In the second method of analysis for the force–calcium loop, we analysed the data in a more dynamic sense by breaking the force–calcium loop into segments (B to C and C to A) as detailed in the Methods section. The B to C segment is described by eqn (3):

$$\text{Force} = Gk_d{}^n \big/ \left(k_d{}^n + [Ca^{2+}]_{IC}{}^n\right) + \text{offset}$$

an empirical fit equation that fits well with force and calcium values in this segment of the force–calcium loop. Figure 7*D* shows that the variable, k_D, that could represent strong crossbridge activation, is significantly increased in both α-TM229 and α-TM276 myofibres when compared to NTG fibres ($P = 0.016$ and $P = 0.047$, respectively). Furthermore, the other variable, n, is significantly decreased only in α-TM276 fibres ($P = 0.0472$). Thus, both TG models display an increase in strong crossbridge activation, which would slow the rates of contraction and relaxation at low levels of calcium activation according to Campbell's model (1997). The C to A segment is best described by the Hill equation (eqn (2):

$$\text{Force} = F_0\left([Ca^{2+}]_{IC}{}^n \big/ k_d{}^n + [Ca^{2+}]_{IC}{}^n\right) + \text{offset}$$

Figure 7*E* shows that k_D increases in α-TM229 fibres ($P = 0.0183$) and decreases in α-TM276 fibres ($P < 0.0001$) compared to NTG fibres. These findings

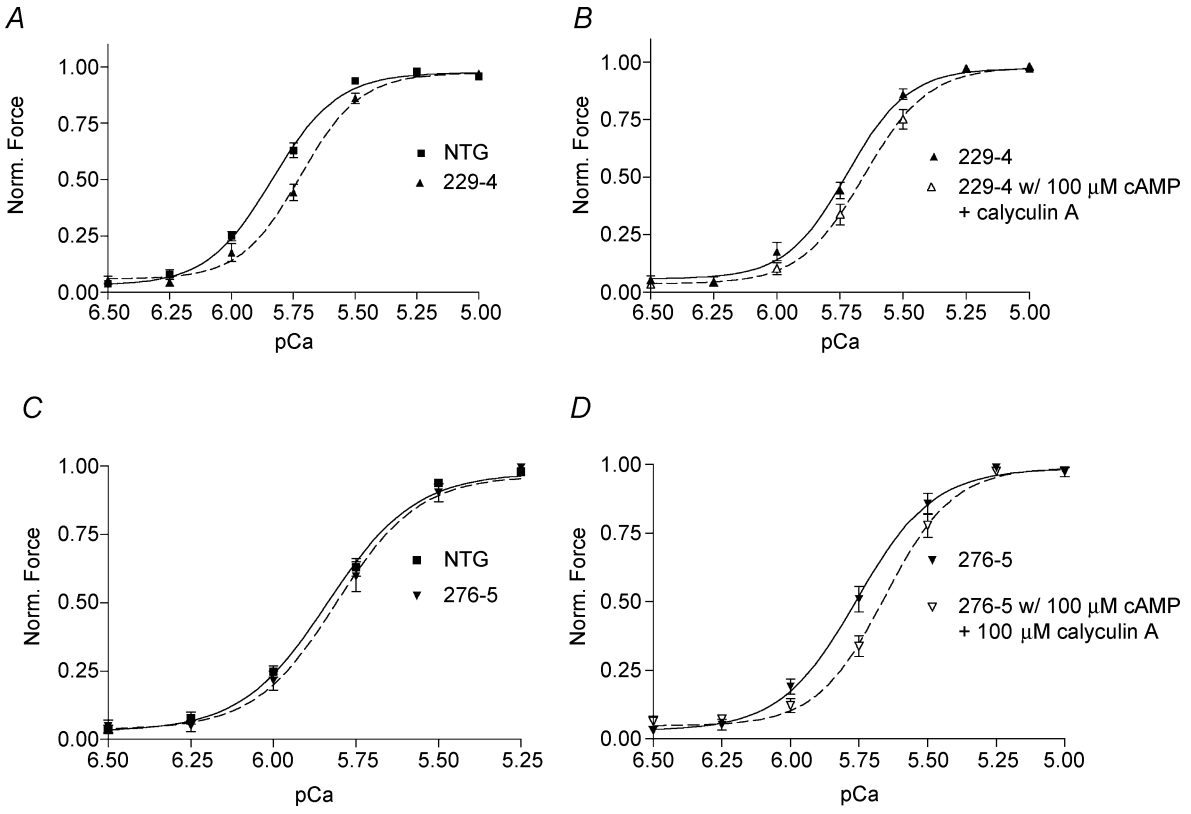

Figure 5. Ca^{2+}–force relationships in skinned fibre papillary bundles from NTG, α-TM229, and α-TM276 male mouse hearts

A and *C*, normalized pCa–force relationship of skinned fibre preparations from (*A*) NTG and α-TM229 and (*C*) NTG and α-TM276 mouse hearts. Force was normalized to the corresponding maximum force at pCa 4.5. Data are presented as mean ± S.E.M. *B* and *D*, normalized pCa-force relation in skinned fibre preparations after cAMP treatment. Note the rightward shifts for both TG preparations after addition of cAMP and the phosphatase inhibitor, calyculin A.

indicate a decrease in calcium sensitivity for α-TM229 fibres during the relaxation phase and an increase in calcium sensitivity for α-TM276 fibres. Furthermore, the other variable, n does not change significantly in both TG fibres when compared to NTG fibres.

α-TM229 and 276 TG hearts do not exhibit any pathological phenotype

Both α-TM229 and α-TM276 TG hearts do not show any obvious phenotypic changes. The heart weight to body weight ratios indicate there is no significant increase in TG

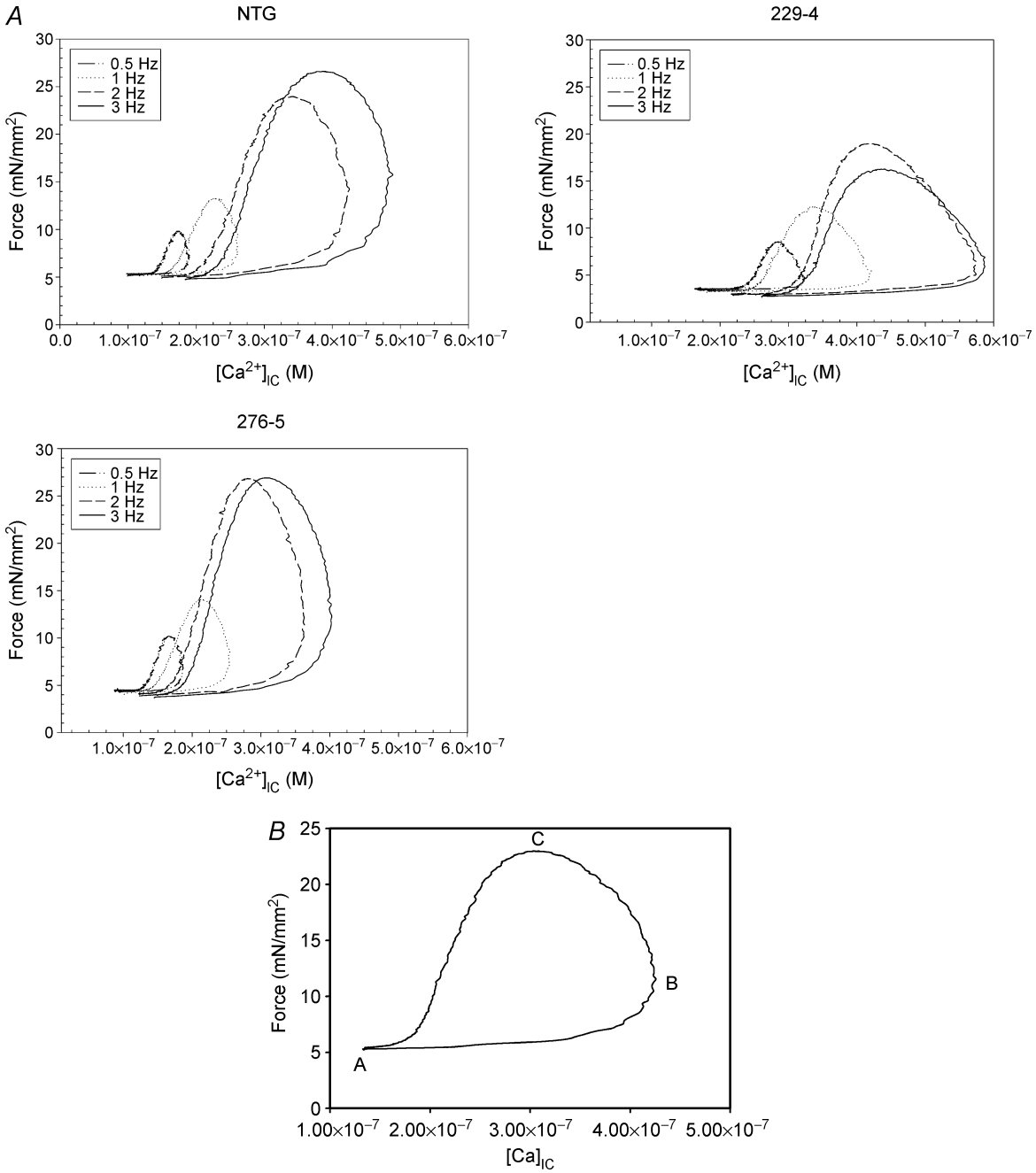

Figure 6. Intact fibre traces and the force-calcium loop
A, force–calcium traces of right ventricular papillary fibres isolated from NTG, α-TM229 and α-TM276 TG male mouse hearts. Both force and $[Ca^{2+}]_{IC}$ increase with increasing stimulation frequency. *B*, example of a force–$[Ca]_{IC}$ loop used in the data analysis. Point A reflects basal levels for force (optimal preload) and $[Ca^{2+}]_{IC}$, B is the point of maximum $[Ca^{2+}]_{IC}$ and the force associated with it while C represents the point of maximum force and its associated $[Ca^{2+}]_{IC}$.

hearts *versus* NTG hearts (4.22 ± 0.067 for NTG, $n = 26$, *versus* 4.26 ± 0.09 and 4.30 ± 0.06 for α-TM229 and 276, $n = 15$, respectively). In addition, extensive histological analyses showed no evidence of anomalies in chamber dimension, fibrosis, inflammation or hypertrophy in these TG hearts when compared to NTG mouse hearts.

Discussion

The data presented here provide the first evidence that specific, charged amino acid residue changes at the inner core and carboxy terminal-end regions of TM have differential effects on cardiac muscle twitch dynamics. In TG α-TM229 hearts, a decrease in both the contractile

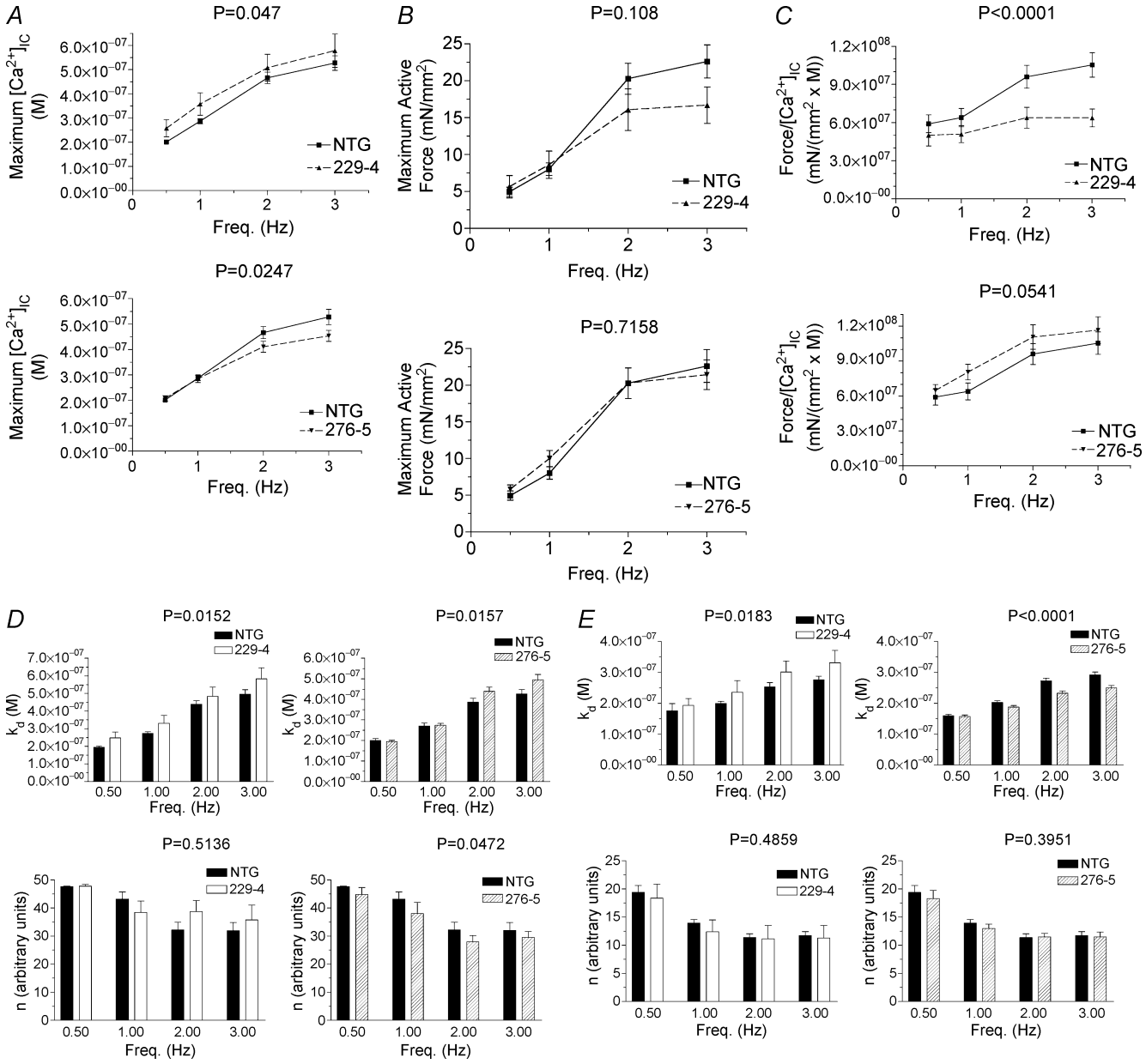

Figure 7. Analyses of the force-calcium loop from membrane-intact α-TM229 TG and α-TM276 TG papillary fibres

All data in this Figure were analysed using a two-way ANOVA with Bonferroni-Dunn's *post hoc* test across the range of frequencies shown (0.5–3 Hz). *P*-values are shown above the graph. Maximum intracellular calcium concentration, $[Ca^{2+}]_{IC}$ (*A*), maximum active force (*B*), and force/$[Ca^{2+}]_{IC}$ (*C*) *versus* frequency is compared between NTG and TG fibres. *D*, the values obtained for the variables, k_D and n, from the data points of the B to C segment are fitted to eqn (3), as described in the Methods section, and compared between NTG and α-TM229 or α-TM276 fibres. *E*, the values obtained for the variables, k_D and n, from the data points of the C to A segment are fitted to eqn (2), as described in the Methods section, and compared between NTG and α-TM229 or α-TM276 fibres.

and relaxation rates in isolated working hearts and a decrease in calcium sensitivity in skinned fibre preparations were observed. Furthermore, these hearts exhibit an increase in strong crossbridge activation and a decrease in calcium sensitivity during the relaxation phase of isolated papillary fibre twitches. The TG α-TM276 mouse hearts exhibited a decrease in the rate of relaxation in isolated working heart preparations and an increase in strong crossbridge activation in isolated papillary fibres. However, they displayed no change in calcium sensitivity in skinned fibres, and they possessed an increase in calcium sensitivity in the relaxation phase of isolated papillary fibre twitches. Since these two residues had different effects on rates of contraction and relaxation, and calcium sensitivity, we propose that the function of TM is compartmentalized along its length.

Residue 229 is found in the inner-core region of TM, portions of which (residues 143–235) have been described as unstable for various reasons (Paulucci *et al.* 2002). The C-terminus of TnT binds to TM within this unstable region, between residues 150 and 180 (White *et al.* 1987), and this region of TnT in turn binds TnI and TnC (Takeda *et al.* 2003). Thus, due to residue 229's proximity to the calcium regulatory switch of the thin filament, TnC, we hypothesize that conformational changes occurring near residue 229 are able to influence calcium sensitivity. This idea is indirectly supported by an earlier biochemical study, which showed that the carboxy terminal end of TnT is sensitive to calcium concentration in the presence of TnC (Pearlstone & Smillie, 1983). In addition, our recent TM structural modelling demonstrated that a charge change at residue 229 causes a local change in the electrostatic potential of TM's surface (Gaffin *et al.* 2004). This charge perturbation also alters the distances between the c-α carbon atoms and carbonyl atoms near the mutated regions of the TM's two monomer strands (Gaffin *et al.* 2004). Thus a portion of the unstable region that is near the TnT–TM interaction site is modified in the α-TM229 molecule. This could alter TM's interaction with either TnT or actin. Taken together, these studies support our finding that a charge alteration at residue 229 is able to decrease myofilament calcium sensitivity.

The data from isolated heart preparations and fibre experiments indicate that mutation at residue 229 in TM molecule primarily impairs systolic function. The decrease in calcium sensitivity in α-TM229 skinned preparations probably explains the decrease in the rate of activation in the working heart preparation for these mice. In addition, no change in the ratio of dP/dt maximum : minimum suggests that there is no independent effect of this mutation on diastolic function. This is further confirmed with no change in τ, a relatively load-independent parameter of diastolic function (Table 1) in α-TM229 hearts compared with NTG hearts. According to Campbell's steady-state model (Campbell 1997), the increase in strong crossbridge activation, i.e. increased constant 'g' that occurs in the B–C segment would also affect the rate of contraction. Furthermore, the data from isolated heart preparations show a significant decrease in TPP in α-TM229 TG hearts, which is consistent with the fibre studies that demonstrate a decrease in myofilament Ca^{2+} sensitivity (Figs 5 and 7*C*). These data also correlate well with the decrease in the slope of the relationship between $+dP/dt$ and work in α-TM229 TG hearts. Taken together our data demonstrate that the mutation at the inner-core region of TM primarily affects the rate of contraction, and the decrease in rate of relaxation observed in the isolated heart preparations could be the consequence of the decrease in rate of contraction.

Residue 276 is located in the carboxyl terminus of TM where contiguous TMs, the N-terminus of TnT, and actin all interact with TM. It has been established that this region of TM, along with the N-terminus of TM, is a primary determinant of actin affinity in the 'open' state (Moraczewska *et al.* 1999; Moraczewska & Hitchcock-DeGregori, 2000) of the three state model (McKillop & Geeves, 1993) of striated muscle contraction. Also, residue 276 is located a considerable distance from TnC; thus, we predict that the effects of the carboxyl terminal region of TM on calcium sensitivity are not as prominent as those of the inner-core region. This is also corroborated by the skinned fibre data, which reveal no change in calcium sensitivity for α-TM276 mouse hearts.

In contrast to the 229 mutation effect, charge alteration at 276 residue in the TM molecule mainly affects the diastolic function that is supported by presented data. Results obtained from the more sensitive intact fibre method show an increase in calcium sensitivity (k_D) for the relaxation phase of the force–calcium loop in α-TM276 TGs. An increase in calcium sensitivity in these mice hearts is also confirmed in Fig. 7, which shows α-TM276 TG fibres achieve the same maximal force as NTG fibres, albeit at a lower calcium concentration. This fact helps explain the decrease in the rate of relaxation found in the working heart preparations of these mice. The decrease in rate of relaxation is also supported by the decrease in τ and in the ratio of $+dP/dt$ to $-dP/dt$ in α-TM276 TG hearts compared with NTGs. TnC stays bound to TnI at lower calcium concentrations, thereby prolonging the transition from the 'open' state of muscle contraction to the 'closed' or 'blocked' state of muscle contraction. In addition, the increase in strong crossbridge activation (k_D) in the B to C segment, i.e. increase in 'g' also exacerbates the rate of relaxation as explained in Campbell's steady-state model (Campbell, 1997). Furthermore, the significant increase in TPP in the isolated heart preparations correlates well with the increase in Ca^{2+} sensitivity at the fibre level in α-TM276 TG hearts. Thus, the data from the isolated heart preparations and the fibre studies demonstrate that

charge change at the carboxy terminal end of TM molecule impairs primarily diastolic function by increasing the myofilament sensitivity to calcium.

One interesting finding is that the effects of these mutant proteins are seen at the higher frequencies (Fig. 7). Our current working hypothesis centres around the phosphorylation of myofibrillar proteins and we have data showing that increasing stimulating frequency causes an increase in the phosphorylation of myosin light chain, myosin binding protein-C (MyBP-C) and Tn I (Tong *et al.* 2004). Tong *et al.* (2004) have recently shown that the effects of MyBP-C and TnI phosphorylation may interact with each other in a coordinated fashion to modulate both the contraction and relaxation phases of the cardiac twitch cycle. We propose that the mutations in the TM molecule could affect its interactions with the neighbouring molecules, actin and Tn complex, and thereby inhibit the aforementioned effects of MyBP-C and TnI phosphorylation. Future studies using pharmacological agents or developing TM TG mouse models with MyBP-C or TnI phosphorylation sites deleted individually or together will further address this possibility.

We have previously shown that exchange of endogenous α-TM with β-TM in the sarcomeres affects the rate of relaxation in work-performing heart studies (Muthuchamy *et al.* 1995), and increases both myofilament calcium sensitivity and the ability of strong crossbridges to activate the thin filament in skinned preparation studies (Palmiter *et al.* 1996). In addition, Wolska *et al.* (1999) found that the rates of contraction and relaxation are depressed in β-TM-containing myocytes compared to NTGs, yet the rate-limiting step of crossbridge detachment is not altered in β-TM hearts. To further understand the mechanisms of altered cardiac contractile parameters in β-TM mice, Jagatheesan *et al.* (2003) have recently shown that TG mice expressing chimeric TM protein (exons 1–8 (residues 1–257) from α-TM plus exon 9 (residues 258–284) from β-TM) exhibit decreased rates of contraction and relaxation in whole heart studies, and a decrease in calcium sensitivity in skinned fibres. Our recent work has replaced amino acids 229 and 276 from α-TM, the residues that are differently charged between α- and β-TM, with their β-TM counterparts (Gaffin *et al.* 2004). Those mouse hearts displayed decreased calcium sensitivity in skinned fibres and a decrease in both the rates of contraction and relaxation in isolated working heart preparations. In the present study, we have sought to discern the effects of individual replacement of these two residues on cardiac function. The importance of these two residues' location (i.e. in the unstable region and carboxy terminal end of TM) in α-TM has been described earlier (Gaffin *et al.* 2004). Our data show that altering these residues in α-TM influences the dynamics of contraction and relaxation by different mechanisms.

An important question from the above-discussed studies is why the different mutations of α-TM or the β-TM protein-containing myofilaments exhibit differential calcium sensitivity. As we have discussed in the α-TMDM paper (Gaffin *et al.* 2004), other amino acids, besides the differences in charged residues, may play a role in determining the variations in cardiac performance and myofilament sensitivity between β-TM TG and α-TM DM TG mice. Although we cannot rule out the possibility that different degrees of TM replacement in α-TM229 and α-TM276 mice (98% *versus* 82%) have varying effects on myofilament calcium sensitivity, our recent studies in another TG line corroborate well with our α-TM276 findings. This TG line in which the last nine amino acids in the carboxy end overlapping region of α-TM (i.e. residues from 276 to 284) is swapped with β-TM residues (approximately 98% replacement) shows no change in calcium sensitivity similar to the α-TM276 myofilaments (R. Gaffin & M. Muthuchamy, unpublished observations). Thus, these data suggest that alterations in the strength of end-to-end interactions of TM could change TM's affinity for actin in the 'open' state of muscle contraction, which affects the kinetics of contraction and relaxation. As we have discussed earlier, the changes in the inner core region of TM could affect the binding of TnT or actin to TM, which in turn could alter the calcium sensitivity of myofilaments. Thus, our data showing the inner core and carboxy terminal overlapping end of TM have differential functions, suggest that the function of TM is compartmentalized along its length.

Taken together, these results provide important insights into the structure–function relationship of TM. First, neither the carboxy terminal end differences (residues 258–284) nor the charged residue changes (residue 229 and 276) between α- and β-TM are solely responsible for the diastolic dysfunction seen in β-TM TG mouse hearts. Other amino acid changes existing between these two isoforms must also contribute to this phenomenon. Second, the various changes in α-TM made in the present study and other studies (Jagatheesan *et al.* 2003; Gaffin *et al.* 2004) impart significant changes in TM structure and function via different means. This points to the fact that perturbations in various regions of TM's semiflexible structure affect its interaction with neighbouring molecules that, in turn, alter sarcomere function.

References

Backx PH & Ter Keurs HE (1993). Fluorescent properties of rat cardiac trabeculae microinjected with fura-2 salt. *Am J Physiol Heart Circ Physiol* **264**, H1098–H1110.

Campbell K (1997). Rate constant of muscle force redevelopment reflects cooperative activation as well as cross-bridge kinetics. *Biophys J* **72**, 254–262.

Gaffin RD, Gokulan K, Sacchettini JC, Hewett TE, Klevitsky R, Robbins J & Muthuchamy M (2004). Charge residue changes in the carboxy-terminus of α-tropomyosin alter mouse cardiac muscle contractility. *J Physiol* **556**, 531–543.

Gao WD, Backx PH, Azan-Backx M & Marban E (1994). Myofilament Ca^{2+} sensitivity in intact versus skinned rat ventricular muscle. *Circ Res* **74**, 408–415.

Grynkiewicz G, Poenie M & Tsien R (1985). A new generation of Ca^{2+} indicators with greatly improved fluorescene properties. *J Biol Chem* **260**, 3440–3450.

Gulick J, Hewett TE, Klevitsky R, Buck SH, Moss RL & Robbins J (1997). Transgenic remodeling of the regulatory myosin light chains in the mammalian heart. *Circ Res* **80**, 655–664.

Guo X, Wattanapermpool J, Palmiter KA, Murphy AM & Solaro RJ (1994). Mutagenesis of cardiac troponin I. Role of the unique NH_2-terminal peptide in myofilament activation. *J Biol Chem* **269**, 15210–15216.

Hibberd MG & Jewell BR (1982). Calcium- and length-dependent force production in rat ventricular muscle. *J Physiol* **329**, 527–540.

Jagatheesan G, Rajan S, Petrashevskaya N, Schwartz A, Boivin G, Vahebi S, DeTombe P, Solaro RJ, Labitzke E, Hilliard G & Wieczorek DF (2003). Functional importance of the C-terminal region of striated muscle tropomyosin. *J Biol Chem* **278**, 23204–23211.

Li L, Desantiago J, Chu G, Kranias EG & Bers DM (2000). Phosphorylation of phospholamban and troponin I in beta-adrenergic- induced acceleration of cardiac relaxation. *Am J Physiol Heart Circ Physiol* **278**, H769–H779.

McKillop DF & Geeves MA (1993). Regulation of the interaction between actin and myosin subfragment 1: evidence for three states of the thin filament. *Biophys J* **65**, 693–701.

McLachlan AD & Stewart M (1975). Tropomyosin coiled–coil interactions: evidence for an unstaggered structure. *J Mol Biol* **98**, 293–304.

McLachlan AD & Stewart M (1976). The 14-fold periodicity in alpha–tropomyosin and the interaction with actin. *J Mol Biol* **103**, 271–298.

Moraczewska J & Hitchcock-DeGregori SE (2000). Independent functions for the N- and C-termini in the overlap region of tropomyosin. *Biochemistry* **39**, 6891–6897.

Moraczewska J, Nicholson-Flynn K & Hitchcock-DeGregori SE (1999). The ends of tropomyosin are major determinants of actin affinity and myosin subfragment 1-induced binding to F-actin in the open state. *Biochemistry* **38**, 15885–15892.

Muthuchamy M, Boivin GP, Grupp IL & Wieczorek DF (1998). β-tropomyosin overexpression induces severe cardiac abnormalities. *J Mol Cell Cardiol* **30**, 1545–1557.

Muthuchamy M, Grupp IL, Grupp G, O'Toole BA, Kier AB, Boivin GP, Neumann J & Wieczorek DF (1995). Molecular and physiological effects of overexpressing striated muscle β-tropomyosin in the adult murine heart. *J Biol Chem* **270**, 30593–30603.

O'Farrell PH (1975). High resolution two-dimensional electrophoresis of proteins. *J Biol Chem* **250**, 4007–4021.

Pagani E & Solaro R (1984). Methods for measuring functional properties of sarcoplasmic reticulum and myofibrils in small samples of myocardium. In *Methods in Pharmacology*, ed. Schwartz A, pp. 49–61. Plenum Publishing Corp, New York, NY.

Palmiter KA, Kitada Y, Muthuchamy M, Wieczorek DF & Solaro RJ (1996). Exchange of β- for α-tropomyosin in hearts of transgenic mice induces changes in thin filament response to Ca2+, strong cross-bridge binding, and protein phosphorylation. *J Biol Chem* **271**, 11611–11614.

Parry DA (1976). Movement of tropomyosin during regulation of vertebrate skeletal muscle: a simple physical model. *Biochem Biophys Res Commun* **68**, 323–328.

Paulucci AA, Hicks L, Machado A, Miranda MT, Kay CM & Farah CS (2002). Specific sequences determine the stability and cooperativity of folding of the C-terminal half of tropomyosin. *J Biol Chem* **277**, 39574–39584.

Pearlstone JR & Smillie LB (1983). Effects of troponin-I plus-C on the binding of troponin-T and its fragments to alpha-tropomyosin. Ca2+ sensitivity and cooperativity. *J Biol Chem* **258**, 2534–2542.

Schachat FH, Bronson DD & McDonald OB (1985). Heterogeneity of contractile proteins. A continuum of troponin–tropomyosin expression in mammalian skeletal muscle. *J Biol Chem* **260**, 1108–1113.

Stewart M & McLachlan AD (1975). Fourteen actin-binding sites on tropomyosin? *Nature* **257**, 331–333.

Subramaniam A, Jones WK, Gulick J, Wert S, Neumann J & Robbins J (1991). Tissue-specific regulation of the alpha-myosin heavy chain gene promoter in transgenic mice. *J Biol Chem* **266**, 24613–24620.

Takeda S, Yamashita A, Maeda K & Maeda Y (2003). Structure of the core domain of human cardiac troponin in the Ca^{2+}-saturated form. *Nature* **424**, 35–41.

Tong CW, Gaffin RD, Zawieja DC & Muthuchamy M (2004). Roles of phosphorylation of myosin binding protein-C and troponin I in mouse cardiac muscle twitch dynamics. *J Physiol* **558**, 927–941.

Walter CA, Nasr-Schirf D & Luna VJ (1989). Identification of transgenic mice carrying the CAT gene with PCR amplification. *Biotechniques* **7**, 1065–1070.

White SP, Cohen C & Phillips GN Jr (1987). Structure of co-crystals of tropomyosin and troponin. *Nature* **325**, 826–828.

Wolska BM, Keller RS, Evans CC, Palmiter KA, Phillips RM, Muthuchamy M, Oehlenschlager J, Wieczorek DF, de Tombe PP & Solaro RJ (1999). Correlation between myofilament response to Ca^{2+} and altered dynamics of contraction and relaxation in transgenic cardiac cells that express β-tropomyosin. *Circ Res* **84**, 745–751.

Acknowledgements

This work is supported by NIH grant HL-60758 to M.M. and NIH grant PO1HL69779 to J.R. The authors acknowledge the NICHD transgenic mouse development facility (contract no. NO1-HD-5-3229) and University of Alabama at Birmingham for generating the transgenic mice. The authors would also like to thank Drs Katalin Kiss and James Samuels for their technical assistance and use of equipment concerning the two-dimensional gel electrophoresis.

Author's present address

C. W. Tong: Department of Internal Medicine, Duke University Medical Center, Durham, North Carolina 27710, USA